NJC

Accepted Manuscript

This is an *Accepted Manuscript*, which has been through the Royal Society of Chemistry peer review process and has been accepted for publication.

Accepted Manuscripts are published online shortly after acceptance, before technical editing, formatting and proof reading. Using this free service, authors can make their results available to the community, in citable form, before we publish the edited article. We will replace this *Accepted Manuscript* with the edited and formatted *Advance Article* as soon as it is available.

You can find more information about *Accepted Manuscripts* in the Information for Authors.

Please note that technical editing may introduce minor changes to the text and/or graphics, which may alter content. The journal's standard Terms & Conditions and the Ethical guidelines still apply. In no event shall the Royal Society of Chemistry be held responsible for any errors or omissions in this *Accepted Manuscript* or any consequences arising from the use of any information it contains.

ROYAL SOCIETY OF CHEMISTRY

www.rsc.org/njc

Cite this: DOI: 10.1039/c0xx00000x

www.rsc.org/xxxxxx

ARTICLE TYPE

A simple approach towards nitrogen-doped graphene and metal/graphene by solid-state pyrolyses of metal phthalocyanine

Wei-Dong Xue and Rui Zhao*

Received (in XXX, XXX) Xth XXXXXXXXX 20XX, Accepted Xth XXXXXXXXX 20XX

DOI: 10.1039/b000000x

Abstract Here we reported a simple and efficient method for the in situ synthesis of nitrogen-graphene and metal/nitrogen-graphene in bulk from pyrolysis of copper phthalocyanine in Ar atmosphere at 800 ^{o}C. By introducing copper foil as the substrates for pyrolysis of organometallic precursors, the rolling up process of graphene sheets into micro/nanoscroll have been observed. We believe that solid-pyrolysis approach opens opportunities for the mass production of graphene based materials at low cost and is useful for applications that need graphene as bulk materials.

1. Introduction

Graphene [1-3], a single atomic layer of sp^2-bonded carbon atoms arranged in a honeycomb lattice, exhibits remarkable electronic, thermal and mechanical properties. The fascinating properties of graphene, such as high surface area (2630 $m^2 \cdot g^{-1}$) [4], high thermal conductivity (~5000 $W \cdot mK^{-1}$) [5], fast charges carrier mobility (~200 000 $cm^2 \cdot V^{-1} \cdot s^{-1}$) [5] and strong Young's modulus (~1 TPa) [6], offer new possibilities for fabricating electronic devices and us as a bulk material. The original mechanical peeling method from highly oriented pyrolytic graphite yields small amounts of high quality graphene [2]. Liquid exfoliation and reduction of graphite oxide have been used to produce chemically converted graphene in large quantities [7, 8]. Annealing SiC, growth from amorphous carbon and CVD has been used to synthesis large-size graphene on wafers [9-11]. However, with regard to liquid exfoliation method, large amount of strong oxidizer, such as sulfuric acid, phosphate acid, and potassium permanganate has been used, which will bring unavoidably serious environmental pollution problems. Chemical vapor deposition (CVD) can be easily scaled up to achieve mass production of the graphene with controlled structures, but a supply of hydrogen to maintain catalyst activity during the high-temperature process (normally above 1000 ^{o}C) is dangerous, while the control of graphene morphology is limited. Furthermore, bulk synthesis of graphene or hetero-atom doping graphene from a simple, controllable, green and low-cost method is still a critical target in scientific and industrial research.

Solid-state pyrolysis of high temperature phthalonitrile resins precursors has recently emerged as an alternative method for preparing carbon nanostructures such as carbon nano tubes (CNTs) and amorphous carbon [12, 13]. Our recent work has shown that solid-state pyrolysis of planar heterocyclic oligmer in a sealed system could provide metal nanowire inside CNTs, however the choice of precursors is critical. Herein, the bulk nitrogen-doped graphene was produced by low temperature solid-state pyrolysis of metal phthalocyanine molecules in a sealed system, which combines this easy method with the inexpensive precursors. Remarkably, the morphology of the graphene can be controlled by inducing different substrates. The rolling up process of graphene sheets into micro/nano-scroll have been observed when a copper foil substrates replaced the ceramic griddle.

The nitrogen-graphene shows different properties compared with the pristine graphene, chemical doping is an important approach to tailor the property of graphene [14, 15]. Similar to the synthesis of nitrogen-CNT, nitrogen-graphene can be obtained through two different ways: direct synthesis and post treatment. Most post treatments may lead to surface doping only. Although in principle, direct synthesis may have the potential to create a homogeneous doping throughout the bulk materials, the results reported so far fail to indicate so.

Metal phthalocyanines are porphyrin derivatives consisting of a central metallic atom bound to π-conjugated nitrogen ligand, the two common bonding configurations, quaternary nitrogen and pyridinic nitrogen, are sp^2 hybridized within the carbon bone, and the mass percent of eight nitrogen atoms in the molecular is above 19 wt%. Considering the simultaneous nitrogen doping though thermal pyrolysis process, it is possible to get a homogeneous nitrogen doping graphene material in bulk.

2. Experimental Section

2.1 Sample preparation: In this manuscript, copper phthalocyanine (CuPc) (30.0 g) was pyrolyzed on ceramic griddle or copper foil substrates at 800 ^{o}C. The heating process was carried under Ar atmosphere (or under H_2/Ar mixture atmosphere with volume ratio of 0.8:9.2) at 5 $^{o}C \cdot min^{-1}$ to 300 ^{o}C (isotherm for 1 h); 5 $^{o}C \cdot min^{-1}$ to 350 ^{o}C (isotherm for 1 h); 5 $^{o}C \cdot min^{-1}$ to 400 ^{o}C (isotherm for 1 h); 3 $^{o}C \cdot min^{-1}$ to 500 ^{o}C (isotherm for 4 h); 2 $^{o}C \cdot min^{-1}$ to 800 ^{o}C (isotherm for 8 h) and then cooled to room temperature naturally. The total time for the synthesis is 22.5 h, and the solid yield was above 20.7 g.

2.2 Samples characterization: The synthesized products were characterized by XRD (Rigaku RINT2400 with Cu Kα

New Journal of Chemistry Accepted Manuscript

radiation), SEM (JSM, 6490LV) and TEM (Tecnai G2 F20 S-TWIN). Raman spectra were collected with Renishaw INVIA Raman System (633 nm laser). The sample used for electromagnetic measurements was prepared by homogeneously mixing with wax in a mass ratio of 4:1. The complex permeability μ ($\mu=\mu'-j\mu''$) and permittivity ε ($\varepsilon=\varepsilon'-j\varepsilon''$) were measured using a vector network analyzer (Agilent 8720ET) at 500M~18GHz.

3. Results and Discussion

Raman spectroscopy has been utilized as a powerful tool for the characterization of graphene, as it can identify the number of layers, the electronic structure, the edge of structure, the type of doping, and any defects in graphene based materials. Figure 1 compared the Raman spectra of CuPc pyrolysised on the ceramic griddle under different atmosphere: H_2/Ar mixture (sample 1) and pure Ar (sample 2). molecular on the ceramic griddle under H_2/Ar mixture (A) and Ar (B).

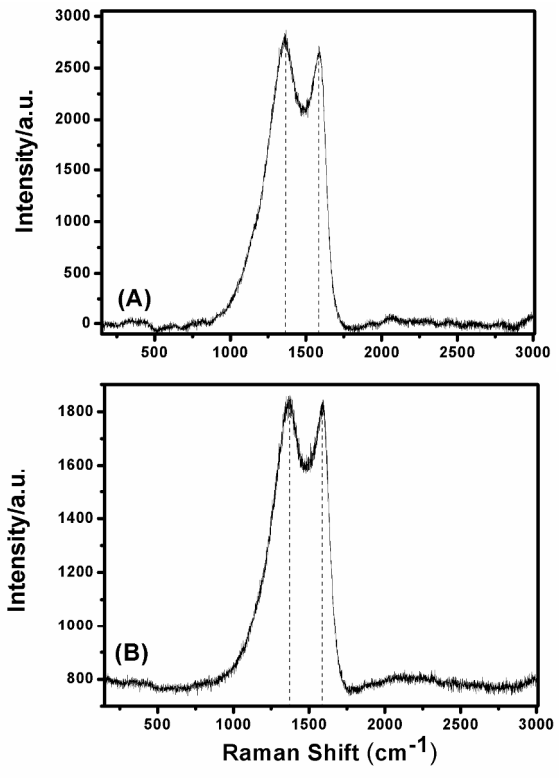

Figure 1 Typical Raman spectra of nitrogen-graphene pyrolysised from CuPc molecular on the ceramic griddle under H_2/Ar mixture (A) and Ar (B).

The Raman spectra of two samples displayed a broad D band peak (the vibrations of carbon atoms with sp^3 electronic configuration of disordered graphene) at 1356 and 1364 cm^{-1} and a G band peak (in-plane vibration of sp^2-bonded atoms) at 1595 and 1587 cm^{-1}. The I_D/I_G ration of the sample 1 was1.07, which was found to be higher than that of the sample 2 (1.01), suggesting a decrease in the average size of the sp^2 domains when the reduction gas H_2 has been used. This may explain why a strong reduction process can increase the number of small domains of aromaticity responsible for the D peak but not affect their overall size, which was related to the G peak. Hydrogen gas was not a good choice in our experiment, so in the following discussion, all the samples from the thermal pyrolysis from CuPc were carried under Ar atmosphere.

To investigate the content of nitrogen atoms, X-ray photoemission spectroscopy (XPS) was performed on the nitrogen-graphene (sample 2). In the survey scan of XPS (see supporting information), the peaks at 284.60 and 398.73 eV correspond to C1s peak of sp^2 carbon and N1s peak of the doped nitrogen, respectively. In the high resolution scan, the asymmetric N1s peak can be divided into two components, indicating that nitrogen atoms were in two different binding states inserted into graphene network: the peak at 398.74 eV corresponds to "pyridinic" nitrogen, and the peak at 401.12 eV was due to quaternary nitrogen in the graphene. The pyridinic nitrogen bonds with two carbon atoms at the edges or defects of graphene and contributes one p electron to the π system; the quaternary nitrogen corresponds to the highly coordinated nitrogen atoms that replaced carbon atoms in the hexagonal ring. Other two peaks appeared at 285.72 and 287.33 eV corresponding to carbon were assigned to the sp^2 and sp^3 carbon atoms, respectively. A small peak at 289.23 eV was ascribed to the physical adsorption of oxygen on the graphene [16, 17]. Generally speaking, the peak at high energy in the C1s spectrum suggested the nitrogen doping occurred in the graphene. Calculated from XPS data, the atomic percentage of nitrogen in the as-obtained nitrogen-doped graphene was found to be ~3.85%. The XPS results along with the D band and G band in the Raman spectra mentioned earlier suggested that the doping nitrogen hetero-atoms have been substituted for carbon atoms in the graphene lattice.

We also made the experiment that CuPc pyrolyzed on copper foil substrates under Ar atmosphere at 800 ^oC (named sample 3). The dispersed materials were investigated by transmission electron microscopy (TEM). In Figure 2A TEM analysis of sample 2 indicated the presence of graphene flakes with lateral size of typically a few nanometers, consisting of several layers. The selected area electron diffraction (SAED) pattern in Figure 2B displayed typical hexagonal crystalline structure of graphene. In Figure 2C and 2D, a wrapped 2D graphene sheet into 1D tubular structure has been observed. The changes of the host's topological structure from planar structure to nanoscroll may share the remarkable mechanical and electronic properties.

Recently, many research groups [18] reported the transformed 2D graphene oxides (GO) nanosheets into carbon nanotubes by sonicating GO in 70% nitric acid, the fact that the graphene sheet could roll itself into a scroll structure under sonication effect. An efficient and controllable way to roll up GO sheets into nanoscrolls was highly enhanced by nanoparticles aggregation [18]. Nanoparticles like Ag, Fe_2O_3 and PdO attached on GO sheets can help the rolling process in a controlled way. Although the rolling mechanism of GO has not been understood comprehensively, it is well-accepted that the oxygen-containing functional groups (carboxyl, carbonyl, hydroxyl and epoxide) exist on the surfaces of GO, which could act as the active sites for the trapping, stabilization, and nucleation of the metal ions [19].

New Journal of Chemistry Accepted Manuscript

This journal is © The Royal Society of Chemistry [year]

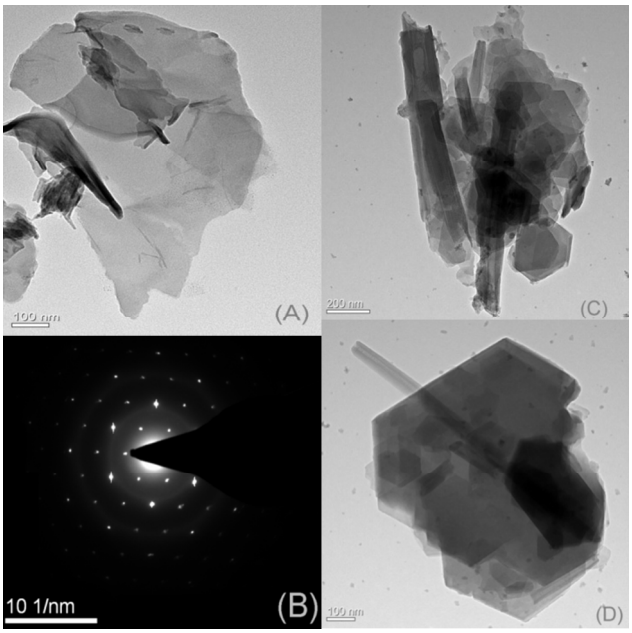

Figure 2 TEM photos showing the nitrogen-graphene pyrolysised from CuPc molecular under Ar atmosphere: (A) pyrolysis from CuPc molecular on the ceramic griddle; (C) and (D) pyrolysised from CuPc molecular on the copper foil; and the magnified image of the rolling grapheme (inside); (B) SAED pattern of nitrogen-graphene pyrolysised from CuPc molecular on the ceramic griddle.

In the present work, different to earlier reports, the pyrolysis process was carried at high temperature under Ar atomosphere, little oxygen-containing functional groups existed. From the X-ray diffraction (XRD) spectra in Figure 3A, the crystal phase of the fabricated sample 2 showed the typical Cu^0 nanoparticles in final material, considering 16 hydrogen atoms in the molecular structure of the CuPc. There was possibility that copper ion has been reduction into copper nanoparticles during the thermal pyrolysis process. Additionally, the copper nanoparticles can be removed from the nitrogen-graphene (sample 2) completely by stirred in HCl solution. From the XRD in Figure 3B, only one broad peak at ~ 26° which belonged to graphene was remained. It was sure that the metal nanoparticles were dispersed in nitrogen-graphene, while, according to the rolling mechanism of GO mentioned in references [18, 19], it may be short of the functional oxygen atoms, and the inefficient action between metal nanoparticles and graphene in rolling the 2D graphene into 1D nanotubes. By introducing copper foil as the substrates for pyrolysis of organometallic precursors, the large amount of copper acted as catalysts in helping the rolling process. Although at present, the detailed mechanism of rolling graphene into nanotubes was not very clear, we could regard the van der Waals forces, the π-π interaction between the substrates metal catalysts and nitrogen-graphene as the factors that contributing the rolling process. If induced functional metal ions, such as Ni^{2+} ions in the organometallic precursors, we also obtained the magnetic nitrogen-doped graphene materials (the XRD spectra see in Figure 4), a typical broad peak at ~ 26° showed the existence of graphene.

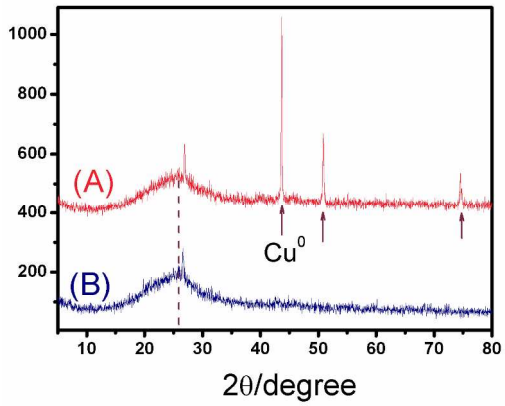

Figure 3 XRD patterns of nitrogen-graphene containing Cu^0 nanoparticles (A); and the pure nitrogen-graphene (B) after the Cu^0 nanoparticles has been removed by HCl.

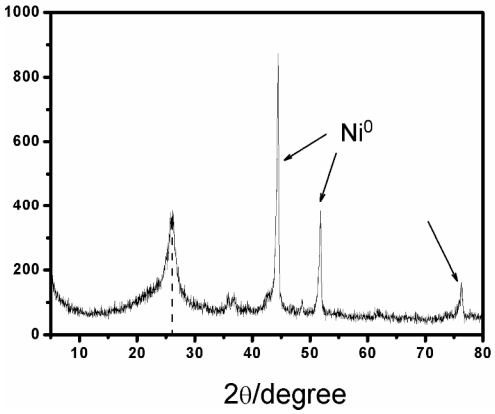

Figure 4 XRD patterns of nitrogen-graphene containing Ni^0 nanoparticles pyrolysised from NiPc molecular on the ceramic griddle under Ar atmosphere at 800 °C.

The EMI SE of a composite material depends mainly on the filler's intrinsic conductivity, dielectric constant, and aspect ratio [20]. Besides the high electrical conductivity, the high surface area and aspect ratio of graphene make it a unique candidate to provide remarkable EMI shielding in polymer composites with light weight [21]. Due to the sp^2 bonded carbon atoms, graphene has high electrical response, but the nitrogen doping graphene showed different properties compared with the pristine graphene. The spin density and charge distribution of carbon atoms will be influenced by the neighbor nitrogen dopants, which induce the "activation region" on graphene surface [22].

Figure 5 showed the frequency dependence of electromagnetic properties of nitrogen-graphene containing Cu^0 nanoparticles (sample 2) and the nitrogen-graphene that Cu^0 nanoparticles has been removed by HCl solution (sample 3). Due to the magnetism was weak, dielectric loss was the main microwave absorbing mechanism of the nitrogen-graphene. Generally, the real parts of relative complex permittivity symbolize the storage ability of electromagnetic energy, and the imaginary parts represent the electromagnetic energy loss ability. From the Figure 5A and 5B, both the Cu^0/nitrogen-graphene (sample 2) and nitrogen-graphene (sample 3) materials showed good permittivity properties, at the

New Journal of Chemistry Accepted Manuscript

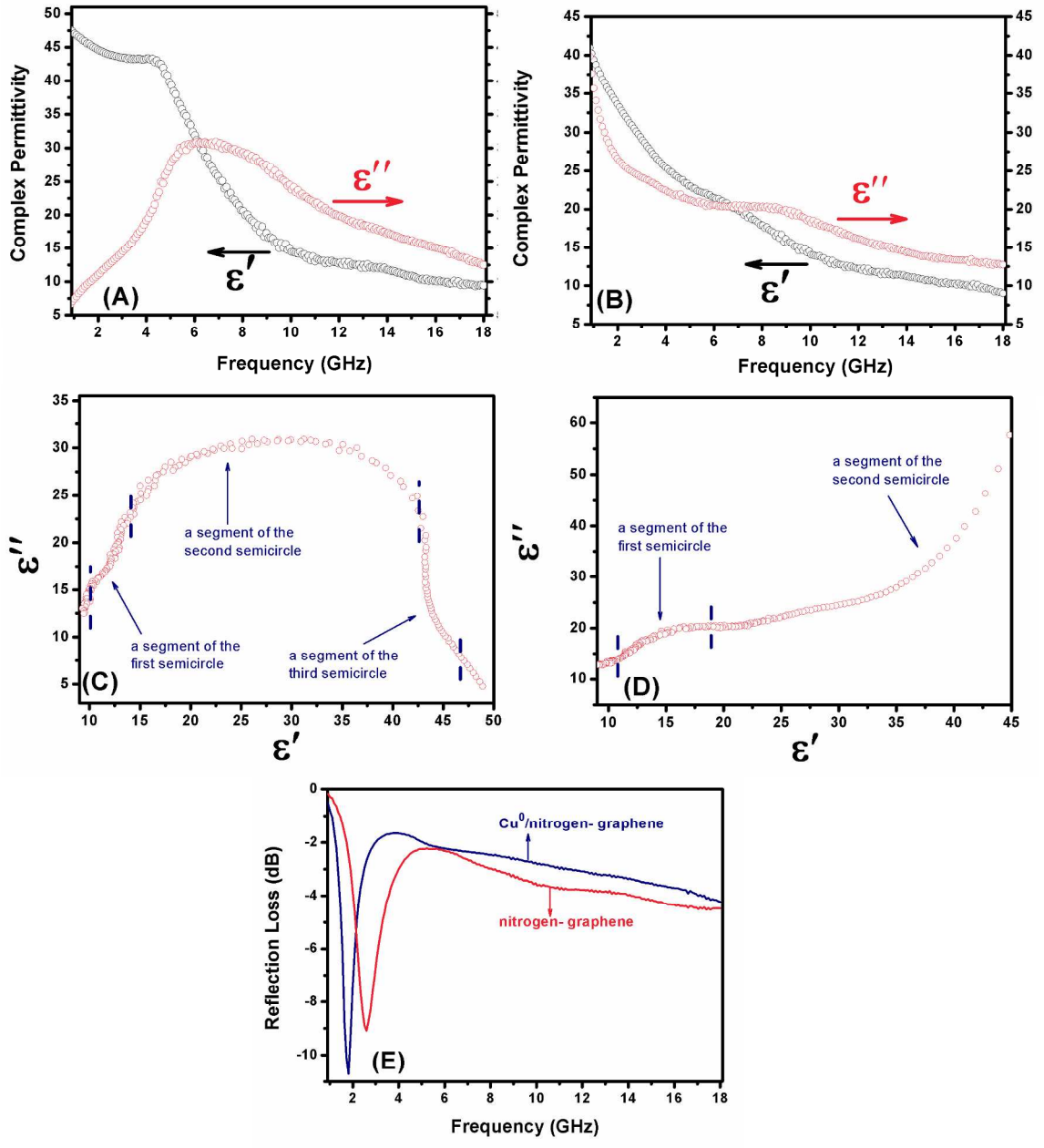

Figure 5 Frequency dependence of relative complex permittivity real part (ε') and imaginary part (ε") of (A) nitrogen-graphene containing Cu^0 nanoparticles; (B) pure nitrogen-graphene; (C) Typical Cole-Cole semicircles (ε" vs ε') for nitrogen-graphene containing Cu^0 nanoparticles; (D) Cole-Cole semicircles (ε" vs ε') for pure nitrogen-graphene; (E) Microwave absorption characteristic of nitrogen-graphene containing Cu^0 nanoparticles and pure nitrogen-graphene at "matching thickness" of 5 mm.

frequency above ~ 6GHz, the values of imaginary parts were even higher than that of the real parts.

First, an important concept relating to microwave absorption was impedance match characteristic, high values of imaginary parts of the nitrogen-graphene based materials will exhibit good microwave absorption: a peak at the C-band with maximum reflection loss was -10 dB (in Figure 5E).

Second, energy transition of microwave band involves the electronic spin, which means greater spin states are required for microwave absorption. It has been documented that localized states near to the Fermi level could be created via introducing lattice defects and electromagnetic energy can be absorbed by the transition from contiguous states to Fermi level when the irradiation is incident on the absorber surface. Moreover, after nitrogen doping in the monolayer graphene, the Fermi level shifts above the Dirac point [23], and the density of state near the Fermi level is suppressed, thus, the band gap between the conduction band and the valence band will be opened. Therefore, the existence of nitrogen atoms in graphene favors the electromagnetic energy absorption, which is another reason why the two samples exhibits better absorbing ability.

Third, for the dielectric loss materials, to absorb electromagnetic wave, relaxation process is also an important reason. Figure 5C and 5D showed the curve characteristic of ε"

This journal is © The Royal Society of Chemistry [year]

New Journal of Chemistry Accepted Manuscript

versus ε', which presented a clear segmet of three overlapped Cole-Cole semicircles for Cu^0/nitrogen-graphene (sample 2) and only two semicircle for nitrogen-graphene (sample 3). This suggested that there was ternary relaxation process for Cu^0/nitrogen-graphene (sample 2) and binary process for nitrogen-graphene (sample 3), with each semicircle corresponding to one Debye relaxation process. The different relaxation process of two samples may arise as following: relaxation process first aroused from delocalized electrons in conductive graphene-based materials, the copper nanoparticles in nitrogen-graphene improving the electric conductive properties of the material, this dielectric relaxation process was obvious and a big Cole-Cole semicircle emerged. Second the defects in the graphene, which can act as polarization centers, with the copper nanoparticles have been removed from the nitrogen-graphene, the partly reconstructed carbon framework, the lag of induced charges were not existence of graphene lattice; therefore, the corresponding Cole-Cole semicircle became smaller. The two semicircles for nitrogen-graphene (sample 3) were mainly from defects in graphene raised by nitrogen atoms.

So the residual defects nitrogen doped graphene can not only improve the impedance match characteristic but also introduce the transition from contiguous states to Fermi level, and defect polarization relaxation favored electromagnetic wave penetration and absorption.

4. Conclusions

We reported a simple and efficient method for the *in situ* synthesis of nitrogen-doped graphene and metal/nitrogen-doped graphene in bulk from the pyrolysis of copper phthalocyanine in Ar atmosphere at 800 ^oC. By introducing copper foil as the substrates for pyrolysis of organometallic precursors, the large amount of copper substrates acted as catalysts in helping rolling the 2D graphene into 1D nanotubes. The Cu^0/nitrogen-graphene materials can be expected to display better absorption than high quality graphene. So we believe that solid-pyrolysis approach opens opportunities for the mass production of graphene based materials at low cost and is useful for applications that need graphene as bulk materials.

Acknowledgements

The work is supported by "the Fundamental Research Funds for the Central Universities, UESTC" (ZYGX2013J034). We also thank Dr. Gui-Ping Yuan of Sichuan University for the TEM measurements and scientific discussions.

Notes and references

[a] *Institute of Applied Electrochemistry, State Key Laboratory of Electronic Thin Films and Integrated Devices, Institute of Microelectronic & Solid State Electronic, University of Electronic Science and Technology of China, Chengdu 610054, P. R. China Email address: ruizhao@uestc.edu.cn (R. Zhao)*

1. A. K. Geim, K. S. Novoselov, The rise of graphene. Nat Mater. 2007; 6(3):183–91.
2. K. S. Novoselov, A. K. Geim, S. V. Morozov, D. Jiang, Y. Zhang, S. V. Dubonos, I. V. Grigorieva, A. A. Firsov, Electric field effect in atomically thin carbon films. Science, 2004, 306 (5296): 666-669.
3. A. K. Geim, Graphene: status and prospects. Science 2009; 324(5934):1530–1534.
4. D. W. Shin, H. M. Lee, S. M. Yu, K. S. Lim, J. H. Jung, M. K. Kim, S. W. Kim, J. H. Han, R. S. Ruoff, J. B.Yoo A facile route to recover intrinsic graphene over large scale. ACS Nano, 2012; 6(9): 7781-7788.
5. A. A. .Balandin Thermal properties of graphene and nanostructured carbon materials. Nat. Mater. 2011; 10 (8):569–81.
6. X. Shen, X. Y. Lin, N. Yousefi, J. J. Jia, J. K. Kim, Wrinkling in graphene sheets and graphene oxide papers. Carbon, 2014; 66: 84-92.
7. Y. Hernandez, V. Nicolosi, M. Lotya, F. M. Blighe, Z. Sun, S. De, I.T. McGovern, B. Holland, M. Byrne, Y. K. Gun'Ko, J. J. Boland, P. Niraj, G. Duesberg, S. Krishnamurthy, R. Goodhue, J. Hutchison, V. Scardaci, A.C. Ferrari, J. N. Coleman. High-yield production of graphene by liquid-phase exfoliation of graphite. Nat. Nanotech., 2008; 3: 563-568.
8. Z. J. Fan, W. Kai, J. Yan, T. Wei, L. J. Zhi, J. Feng, Y. M. Ren, L. P. Song, F. Wei, Facile synthesis of graphene nanosheets via Fe reduction of exfoliated graphite oxide. ACS Nano, 2011; 5(1): 191-198.
9. H. J. Ji, Y. Hao, Y. Ren, M. Charlton, W. Lee, Q. Wu, H. Li, Y. Zhu, Y. Wu, R. Piner, R. S. Ruoff, Graphene growth using a solid feedstock and hydrogen. ACS Nano, 2011; 5(9):7656-7661.
10. Z. Sun, Z. Yan, J. Yao, E. Beitler, Y. Zhu, J. M. Tour, Growth of graphene from solid carbon sources. Nature, 2010; 468: 549-552.
11. N. Liu, L. Fu, B. Dai, K. Yan, Z. Liu, Universal segregation growth approach to wafer-size graphene from non-noble metals. Nano. Lett., 2011; 11: 297-303.
12. (a) R. Zhao, Y. Lei, Y. Zhan, F. Meng, K. Jia, J. Zhong, X. Liu, Solid-state pyrolysis of iron phthalocyanine polymer into iron nanowire inside carbon nanotube and their novel electromagnetic properties J. Mater. Res., 2011; 26(18): 2369-2372. (b) Y. Lei, R. Zhao, Y. Zhan, F. Meng, J. Zhong, X. Yang, X. Liu, Generation of multiwalled carbon nanotubes from iron–phthalocyanine polymer and their novel dielectric properties. Chem. Phys. Lett., 2010; 496 (1-3):139-142.
13. (a) M. Gao, S. Huang, L. Dai, G. Wallance, R. Gao, Z. Wang. Aligned coaxial nanowires of carbon nanotubes sheathed with conductiong polymer. Angew. Chem. Int, Ed., 2000; 39: 3664-3666.(b) L. Zhi, T. Gorelik, R. Friedlein, J. Wu, U. Kolb, W. R. Salaneck, K. Müllen, Solid-State Pyrolyses of Metal Phthalocyanines: A Simple Approach towards Nitrogen-Doped CNTs and Metal/Carbon Nanocable. Small, 2005; 1:798-801. (c) M. Laskoski, T. M. Keller, S. B. Qadri, Direct conversion of highly aromatic phthalonitrile thermosetting resins into carbon nanotubes containing solids. Polymer 2007; 48: 7484-7489.
14. Y. Shao, S. Zhang, M. H. Engelhard, G. Li, G. Shao, Y. Wang, J. Liu, I. Aksay, Y. Lin, Nitrogen-doped graphene and its electrochemical applications. J. Mater. Chem., 2010; 20: 7491-7496.
15. C. P. Ewels, M. Glerup, Nitrogen doping in carbon nanotubes. Nanosci. Nanotechnol., 2005; 5: 1345-1363.
16. Z. H. Sheng, L. J. Shao, J. Chen, W. J. Bao, F. B. Wang, X. H. Xia, Catalyst-Free Synthesis of Nitrogen-Doped Graphene via Thermal Annealing Graphite Oxide with Melamine and Its Excellent Electrocatalysis. ACS Nano, 2011; 5: 4350-4358.
17. H. Wang, T. Maiyalagan, X. Wang, Review on recent progress in nitrogen-doped graphene: synthesis, characterization, and its potential applications. ACS Catalysis, 2012; 2: 781-794.
18. (a) T. Sharifi, E. Gracia-Espino, H. R. Barzegar, X. Jia, F. Nitze, G. Hu, P. Nordblad, C. W. Tai, T. Wagberg, Formation of nitrogen-doped graphene nanoscrolls by adsorption of magnetic γ-Fe_2O_3 nanoparticles. Nat. Commun., 4, doi:10.1038/ncomms3319; (b) X. Wang, D. P. Yang, G. Huang, P. Huang, G. Shen, S. Guo, Y. Mei, D. Cui, Rolling up graphene oxide sheets into micro/nanoscrolls by nanoparticle aggregation. J. Mater. Chem. 2012; 22: 17441–17444; (c) M. Quintana, M. Grzelczak, K. Spyrou, M. Calvaresi, S. Bals, B. Kooi, G. V. Tendeloo, P. Rudolf, F. Zerbetto, M. Prato, A simple road for the transformation of few-layer graphene into MWNTs J. Am. Chem. Soc., 2012; 134:13310–13315; (d) S. Wang, L. A. Tang, Q. Bao, M. Lin, S. Deng, B. M. Goh, K. P. Loh, Room-Temperature Synthesis of Soluble Carbon Nanotubes by the Sonication of

New Journal of Chemistry Accepted Manuscript

Graphene Oxide Nanosheets. J. Am. Chem. Soc., 2009; 131: 16832–16837.

19. (a) G. Xiang, J. He, T. Li, J. Zhuang, X. Wang, Rapid preparation of noble metal nanocrystalsvia facile coreduction with graphene oxide and their enhanced catalytic properties. Nanoscale, 2011; 3: 3737-3742; (b) R. Pasricha, S. Gupta, A. K. Srivastava, A facile novel synthesis of Ag-graphene-based nanosomposites. Small, 2009; 5: 2253-2259.
20. N. Li, Y. Huang, F. Du, X. He, X. Lin, H. Gao, Electromagnetic interference (EMI) shielding of single-walled carbon nanotube epoxy composites. Nano Lett 2006;6:1141–5.
21. (a) M. H. Al-Saleh, U. Sundararaj, Electromagnetic interference shielding mechanism of CNT/polymer composites. Carbon 2009; 47:1738–46. (b) S. T. Hsiao, C. C. M. Ma, H. W. Tien, W. L. Liao, Y. S. Wang, S. M. Li, Y.C. Huang , Carbon 2013. 60: 57-66.
22. Y. Kang, Z. Y. Chu, D. J. Zhang, G.Y. Li, Z. H. Jiang, H. F. Cheng, X. D. Li, Incorporate boron and nitrogen into graphene to make BCN hybrid nanosheets with enhanced microwave absorbing properties. Carbon 2013; 61:200-208.
23. (a) M. Wu, C. Gao, J. Z. Jiang, Light non-metallic atom (B, N, O and F)-doped graphen: a first-principles study. Nanotechnology, 2010; 21: 505202; (b) D. Wei, Y. Liu, Y. Wang, H. Zhang, L. Huang, G. Yu, Synthesis of N-doped graphene by chemical deposition and its electrical properties. Nano Lett., 2009; 9: 1752-1758.

New Journal of Chemistry Accepted Manuscript

This journal is © The Royal Society of Chemistry [year]